XLVI CILAMCE
VITÓRIA - ES - BRAZIL - 2025
XLVI IBERO-LATIN AMERICAN CONGRESS ON COMPUTIONAL METHODS IN ENGENEERING

Design of Rectangular Concrete-Filled Steel Tube (RCFT) Columns of Noncompact and Slender Section

Glaubert A. Miranda[1], Rodrigo S. Camargo[2], Adenilcia F. G. Calenzani[3], Walnório G. Ferreira[4]

[1234]Dept. of Civil Engineering, Federal University of Espírito Santo
Avenida Fernando Ferrari, 514, 29.075-910, ES/Goiabeiras. Vitória
glaubert.miranda@edu.ufes.br, rodrigo_camargo2000@yahoo.com adenilcia.calenzani@ufes.br, walnorio@gmail.com

Abstract. Concrete-filled steel tubular (CFT) columns have gained prominence in structural projects due to their high strength, stiffness and combined bending and compression performance. In Brazil, NBR 8800:2024 introduced provisions for the combined bending and compression design of noncompact and slender sections through Calculation Models I and III. This study presents a computational tool developed in MATLAB to verify the combined bending and compression resistance of rectangular composite filled columns, based on the formulations of the NBR 8800:2024. According to the normative stress diagrams, the neutral axis was determined by force equilibrium, applying the secant method for noncompact sections and the quadratic formula for slender sections, while the resistant moments were obtained by moment equilibrium. The normative procedures were evaluated by comparison with experimental results reported in the literature. The findings showed reasonable agreement with the experimental data, with a conservative trend in the assessed cases. However, the scarcity of tests involving noncompact and slender sections still limits a broader assessment of the normative models, highlighting the need for further experimental studies.

Keywords: Composite columns, combined bending and compression, noncompact section, slender section, NBR 8800:2024.

1 Introduction

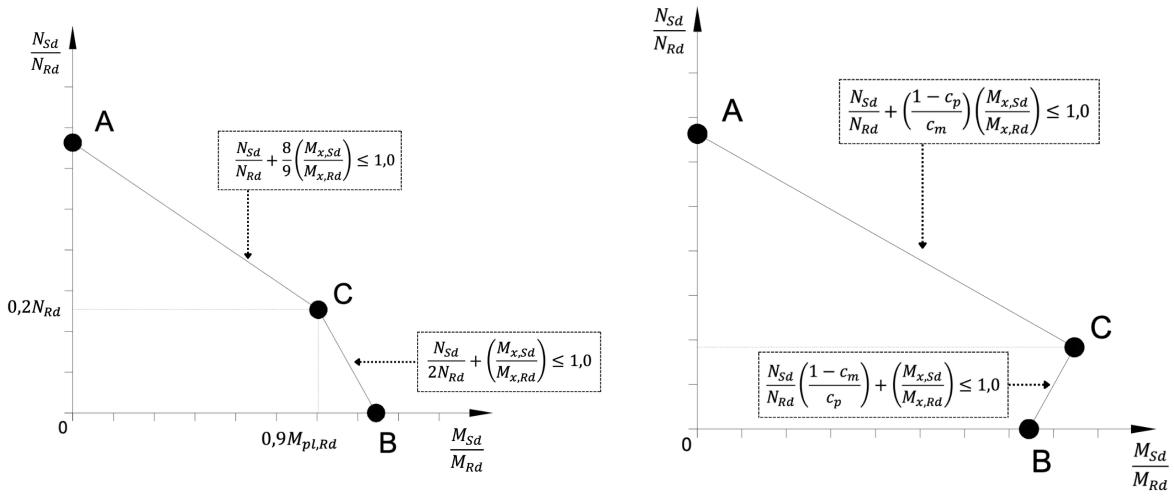
Concrete-filled steel tube (CFT) columns, particularly those with rectangular cross-sections (RCFT), have been increasingly recognized as efficient structural solutions due to their high load-carrying capacity and enhanced performance under combined bending and compression. As demonstrated by Zhichao Lai, Amit Varma, and Kai Zhang [1], this type of member can exhibit superior structural behavior compared to stand alone steel or reinforced concrete members, resulting from the interaction between the steel tube and the concrete core. The steel profile provides lateral confinement to the concrete, increasing its compressive strength, while the concrete, in turn, helps delay local buckling of the steel tube walls. In this context, several international studies have sought to improve design criteria for composite tubular columns. Wenbing Han and Ying Wang [2] highlight that codes such as AISC 360-22 [6], Eurocode 4 [7], and the Chinese code GB 50936 [8] incorporate broader provisions, including detailed classifications of compact sections, noncompact, and slender, as well as allowing the use of high-strength materials that exceed the limits established by Brazilian codes. Complementing this analysis, Cintia Ibáñez, David Hernández-Figueirido, and Adrián Piquer [3] demonstrated that, even among international codes, the results can range from conservative to non-conservative depending on the steel thickness and the concrete strength.

Beyond experimental contributions, analytical advances have also been significant. Zhichao Lai and Amit Varma [4] demonstrated, through three-dimensional finite element models, that the use of specific stress–strain relationships is essential to accurately predict the behavior of noncompact and slender members. These relationships enable the proper representation of phenomena such as local buckling, concrete nonlinearity, lateral confinement, and circumferential stresses, factors often overlooked in simplified approaches adopted by current

codes.

In Brazil, the design of concrete-filled rectangular composite tubes (RCFT) still relies on simplified models prescribed by ABNT NBR 8800:2024 [5]. This code limits its application to concrete with a characteristic compressive strength of up to 50 MPa and steel tubes with a yield strength not exceeding 450 MPa. Until the 2024 revision, NBR 8800 addressed only sections classified as compact, with no specific provisions for the design of noncompact and slender sections. Only with this most recent revision did the code incorporate design criteria for these classifications, significantly expanding its scope of application.

In this study, only materials whose properties comply with the limits established by Brazilian codes are adopted, ensuring conformity with current prescriptions. The latest edition of NBR 8800 [5] introduces two distinct approaches for verifying the resistance of noncompact and slender sections, Calculation Models I and III, both inspired by the criteria established by the American code AISC 360-22 [6]. These models can be represented, in a simplified form, by an N-M interaction curve composed of two linear segments, AC and CB, that form a polygonal line, as illustrated in Fig. 1.



(a) Diagram MN – Model I (b) Diagram MN – Model III

Figure 1. Combined bending and compression diagram of calculation Models I and III

To apply the verification models for combined bending and compression, it is necessary to determine the resistant bending moment and axial load of the composite column. ABNT NBR 8800:2024 [5] provides, for this purpose, specific equations for calculating the resistant moment, differentiated according to the cross-section classification noncompact or slender. For noncompact sections, the resistant capacities are determined by Equations (1) and (2):

$$N_{p,Rd} = N_{pl,Rd} - \frac{N_{pl,Rd} - N_{y,Rd}}{\left(\lambda_r - \lambda_p\right)^2}\left(\lambda - \lambda_p\right)^2 \tag{1}$$

$$M_{p,Rd} = M_{pl,Rd} - \left(M_{pl,Rd} - M_{e,Rd}\right)\frac{\left(\lambda - \lambda_p\right)}{\left(\lambda_r - \lambda_p\right)} \tag{2}$$

For slender sections, the code establishes the following equations:

$$N_{p,Rd} = \sigma_{cr,Rd}A_a + f_{cd2}\left(A_c + A_s\frac{E_s}{E_c}\right) \tag{3}$$

$$M_{p,Rd} = M_{cr,Rd} \tag{4}$$

Where $N_{p,Rd}$ and $M_{p,Rd}$ are, respectively, the design axial resistance and the design bending moment resistance of the composite column, and $\lambda, \lambda_p, \lambda_r, \lambda_{max}$, are the slenderness parameters given in Table M.1 of NBR

8800:2024 [5]. However, it is noted that the code does not provide explicit equations for calculating the bending moment corresponding to the onset of compression plastification ($M_{e,Rd}$) in noncompact sections, nor for the moment corresponding to the initiation yield in the tension flange of the steel tube ($M_{cr,Rd}$) in slender sections. Instead, NBR 8800:2024 [5] presents specific stress diagrams that must be used as the basis for determining the position of the neutral axis, a necessary step to obtain $M_{e,Rd}$ and $M_{cr,Rd}$. These diagrams describe the stress distribution in the different materials comprising the composite section the steel tube, the concrete core, and any additional longitudinal reinforcement when present and are shown in Figs. 2 and 3, adapted by the author based on the original representations from the code.

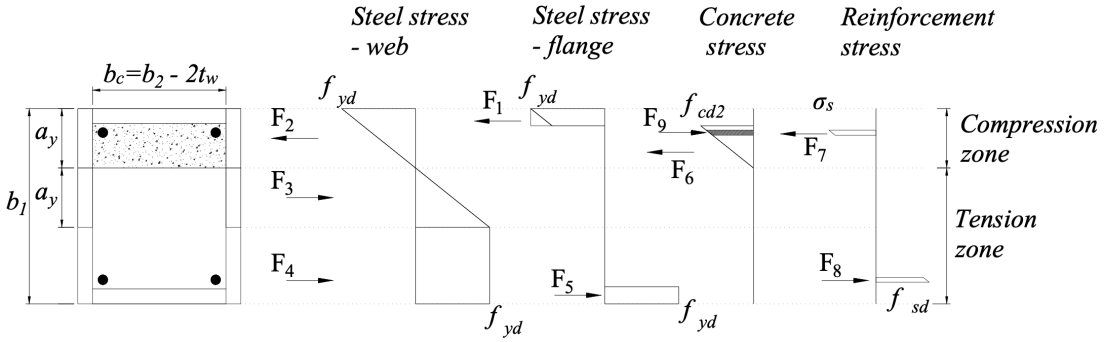


Figure 2. Noncompact section

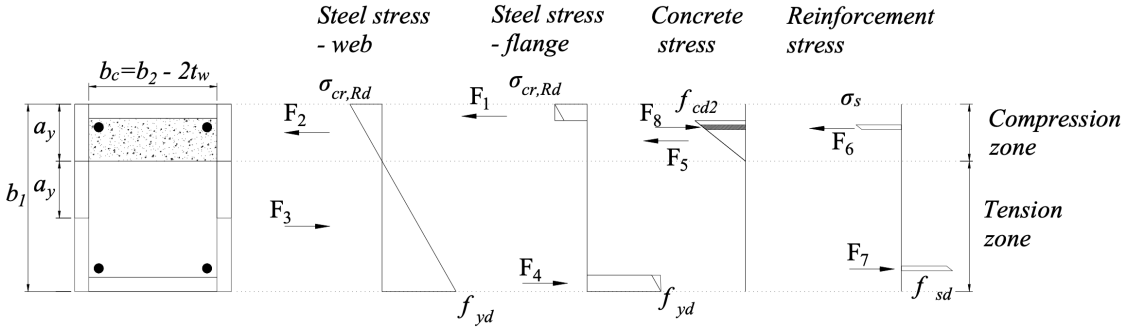


Figure 3. Slender section

This study aims to address existing gaps in the application of normative models to the combined bending and compression of noncompact and slender sections by proposing a computational tool based on NBR 8800:2024 [5], which employs the secant method and the quadratic formula to determine the position of the neutral axis for obtaining, respectively, the moment corresponding to the onset of compression plastification ($M_{e,Rd}$) noncompact sections and the moment corresponding to the yield initiation in the tension flange of the steel tube ($M_{cr,Rd}$) in slender sections.

2 Design of Concrete-Filled Steel Tube Composite Columns According to NBR 8800:2024

Calculation Model I, as presented in NBR 8800:2024 [5], is based on the methodology of the American code AISC 360–22 [6], adopting the same resistance verification criteria used for steel columns subjected to combined bending and compression. The verification of the interaction between axial forces and bending moments is performed through specific expressions that define the safety condition of the cross-section. These expressions, applicable to biaxial bending, are given by Equations (1) and (2).

For $\frac{N_{Sd}}{N_{Rd}} \geq 0.2$:

$$\frac{N_{Sd}}{N_{Rd}} + \frac{8}{9}\left(\frac{M_{Sd}}{M_{Rd}}\right) \leq 1.0 \tag{5}$$

For $\frac{N_{Sd}}{N_{Rd}} < 0.2$:

$$\frac{N_{Sd}}{2N_{Rd}} + \left(\frac{M_{Sd}}{M_{Rd}}\right) \leq 1.0 \tag{6}$$

The graphical representation of these expressions gives rise to the bilinear interaction diagram of axial force versus bending moment shown in Fig. 1, characteristic of uniaxial bending situations. When the sum of the terms on the left-hand side of the equations results in a value lower than 1.0, the section is in a safe condition. If the value equals 1.0, the corresponding point lies on the resistance surface, representing the safety limit. Values greater than 1.0, however, indicate that the section has exceeded the predicted resistance capacity. Calculation Model III, also based on AISC 360–22 [6], is specifically aimed at the design of noncompact composite column noncompact sections and slender and adopts a different approach for verifying combined resistance. The expressions used are presented in Equations (3) and (4).

For $\frac{N_{Sd}}{N_{Rd}} \geq c_p$;

$$\frac{N_{Sd}}{N_{Rd}} + \left(\frac{1 - c_p}{c_m}\right)\left(\frac{M_{Sd}}{M_{Rd}}\right) \leq 1{,}0 \tag{3}$$

For $\frac{N_{Sd}}{N_{Rd}} < c_p$;

$$\frac{N_{Sd}}{N_{Rd}}\left(\frac{1 - c_p}{c_m}\right) + \left(\frac{M_{Sd}}{M_{Rd}}\right) \leq 1{,}0 \tag{4}$$

In these equations, the coefficients c_m and c_p are defined as a function of the geometry and the section classification (noncompact or slender), adjusting the interaction response between axial force and bending moment for concrete-filled rectangular sections. Fig. 2 graphically illustrates these relationships for the case of bending with respect to one of the principal axes of the section.

2.1 Calculation Procedure for Bending Resistance

For the calculation of the combined bending and compression resistance of concrete-filled composite tubular columns, the principle of static equilibrium was adopted as the basis for determining the position of the neutral axis, using the stress diagrams presented in NBR 8800:2024 [5]. Once this position was identified, the corresponding moments were obtained, which are necessary to calculate the bending moment associated with the onset of compression plastification and the moment corresponding to the yield initiation in the tension flange of the steel profile. Initially, the resistant force of each material steel tube, concrete, and longitudinal reinforcement was determined based on the stress distributions defined by the code (Figs. 2 and 3). From these forces, the equilibrium equation was formulated by imposing that the algebraic sum of the internal tensile and compressive forces be equal to zero. In the case of noncompact sections, to solve the force equilibrium equation, the secant numerical method was applied, using two initial guesses for the position of the neutral axis and a limit of up to 1,000 iterations, as defined by user parameters. The iterative process yielded the depth of the neutral axis that satisfies the equilibrium condition, allowing for the calculation of the bending moment corresponding to the onset of compression plastification ($M_{e,Rd}$). It is noteworthy that this procedure was adopted exclusively for noncompact sections, whose bending moment resistance is not directly provided by the code, therefore requiring a numerical approach.

In the case of slender sections, the formulation of the internal force equilibrium equation, based on the normative stress distribution, resulted in a quadratic equation with respect to the depth of the neutral axis. This allowed for the direct application of the quadratic formula to determine its position, eliminating the need for iterative procedures. Once this depth was obtained, it was possible to calculate the moment corresponding to the

yield initiation in the tension flange of the steel profile ($M_{cr,Rd}$).

3 Computational Implementation

The expressions used in the verification process were implemented in MATLAB [10] to automate the calculations and enable efficient analysis of different sections. The developed tool performs the determination of the neutral axis, the calculation of the resistant forces, and the verification of combined bending and compression in accordance with the normative models. The program also allows for the adjustment of parameters such as the initial values for the neutral axis position and the maximum number of iterations, providing flexibility in the calculation process.

To verify the reliability of the developed tool, a validation procedure was carried out in which rectangular tubular sections available in the technical catalogs of manufacturers TUPER and PROTUBSA were analyzed. Columns numbered from 1 to 5, classified as noncompact and slender sections with varying dimensions, as shown in Table 1, were calculated considering a length of 300 cm, concrete with a characteristic compressive strength of 50 MPa, steel profiles with a yield strength of 355 MPa, and four longitudinal bars with a nominal diameter of 12.5 mm made of CA50 steel.

Table 1. Properties of the profiles extracted from the catalog

Manufacturer	Columns	b_1 (mm)	b_2 (mm)	t (mm)
TUPER [12]	1	250	100	3.75
	2	250	100	4.25
	3	300	100	3.75
	4	300	100	4.25
PROTUBSA [13]	5	500	300	8

Using the computational tool, the resistant moments of the x- and y-axes ($M_{Rd,x}$ e $M_{Rd,y}$), the axial resistance (N_{Rd}), and the steel contribution factor (δ) defined by NBR 8800:2024 [5] were determined. This factor classifies the columns according to the contribution of the materials: for $\delta < 0.1$, the column must be designed as a concrete column according to NBR 6118 [14]; for $\delta > 0.9$, the column must be verified as a steel column according to NBR 8800 [5]; and for intermediate values, the column is considered composite, following the criteria of NBR 8800 [5]. The results obtained for composite columns with the sections described in Table 1 are presented in Table 2. It is observed that, for all the profiles analyzed, $M_{Rd,x}$ is greater than $M_{Rd,y}$ due to the higher moment of inertia about the x-axis. Profiles classified as compact about the x-axis become noncompact or slender about the y-axis, as in column 3, demonstrating that the section classification depends on the bending axis direction. Regarding the δ factor, all columns presented in Table 2 can be designed as composite.

Table 2. Results of the commercial profiles

	Bending of the x-axis		Bending of the x-axis		Axial force and contribution factor	
Columns	$M_{Rd,x}$ (kN.cm)	Section classification	$M_{Rd,y}$ (kN.cm)	Section classification	N_{Rd} (kN)	δ
1	7877.79	Compact	4019.76	Noncompact	1273.13	0.5304
2	8737.26	Compact	4289.67	Noncompact	1286.83	0.5642
3	10772.70	Noncompact	5401.05	Slender	1472.18	0.5208
4	11869.69	Compact	5202.40	Noncompact	1555.00	0.5546
5	82168.38	Compact	53888.62	Noncompact	7827.14	0.4893

Table 3 presents the ratio between the results provided by the developed tool and those obtained through the

manual resolution of the design equations, with the plastic neutral axis determined using MATHEMATICA [10]. The values indicate that the computational tool consistently calculates the normative parameters for commercial profiles, as the deviations from the manual calculation are equal to or less than 0.125%.

Table 3. Ratio between the results obtained by the tool and those from the manual calculation

Columns	$M_{Rd,x,software}/M_{Rd,x,manual}$	$M_{Rd,y,software}/M_{Rd,y,manual}$	$N_{Rd,software}/N_{Rd,manual}$
1	0.125%	0.118%	0.002%
2	0.113%	0.105%	0.015%
3	0.000%	0.004%	0.003%
4	0.083%	0.012%	0.002%
5	0.012%	0.018%	0.005%

4 Results and Discussion

After validating the developed tool, a critical analysis of the provisions of NBR 8800:2024 [5] for combined bending and compression verification was carried out by comparing the results provided by the tool with experimental data obtained from full-scale tests reported in the literature. The specimen previously tested by Uy [9] were used. This procedure allowed for an assessment of the consistency of the normative models against experimental data. Table 4 presents the properties of the specimen, highlighting the experimental values of axial load and ultimate moment N_u and M_u, as well as the corresponding section classification according to the criteria of NBR 8800:2024 [5].

Table 4. Properties of the specimen extracted from the literature

Reference	Specimen name	b (mm)	t (mm)	f_y (MPa)	f_c (MPa)	N_u (kN)	M_u (kN.cm)	L (mm)	Section classification
Uy [9]	NS2	186	3	300	32	1069	3960	540	Noncompact
	NS3	186	3	300	32	1133	6340	540	
	NS4	186	3	300	32	895	7520	540	
	NS8	246	3	300	38	2255	10820	720	Slender
	NS9	246	3	300	38	1900	14060	720	
	NS10	246	3	300	38	1279	12790	720	

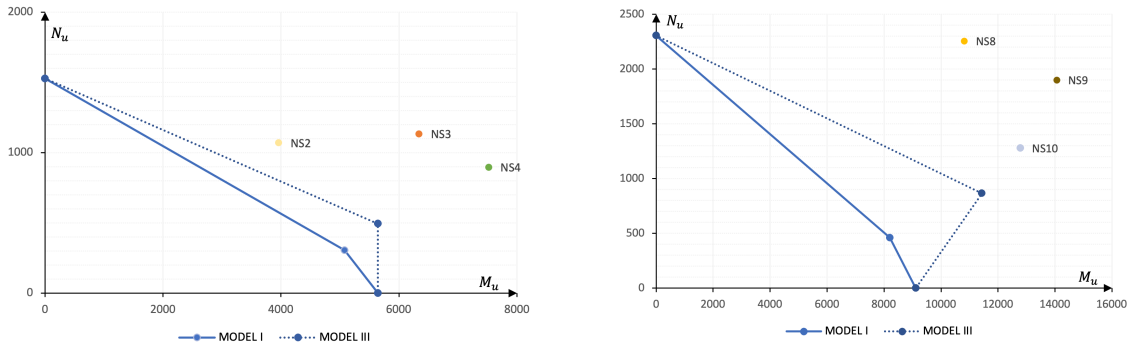
In the analysis implemented by the tool, for axial loading, the ultimate axial load from the test N_u was considered as input, and the maximum bending moment that, together with this axial load, would satisfy the normative interaction expression was determined. Table 5 presents the comparison between the resistant moments obtained using Calculation Models I and III, implemented in the tool, and the experimental values reported by Uy [9], for specimen with noncompact sections (NS2, NS3, and NS4) and slender sections (NS8, NS9, and NS10).

For the noncompact specimen, the results show that Model III reproduced the resistance observed in the tests more accurately, with M_{max}/M_u ratios ranging from 0.288 to 0.537, while Model I provided more conservative estimates, ranging from 0.258 to 0.481. This difference was already expected, since Model I follows the same interaction curve applied to purely steel members, whereas Model III incorporates adjustments to account for the concrete contribution, albeit still conservatively. For the slender specimen, however, the discrepancies were more significant. In NS8, for instance, Model I yielded a ratio of only 0.021, and Model III, although slightly higher, reached only 0.031.

Table 5. Results comparing the normative models and the specimen

	Experimental data		Resistance according to NBR 8800:2024		Maximum moment obtained from the interaction equation		Comparison: Code *versus* Experiment	
Specimen name	N_u (kN)	M_u (kN.cm)	N_{Rk} (kN)	M_{Rk} (kN.cm)	Model I M_{max} (kN.cm)	Model III M_{max} (kN.cm)	Model I M_{max}/M_u (kN.cm)	Model III M_{max}/M_u (kN.cm)
NS2	1069	3960			1904.67	2126.40	0.481	0.537
NS3	1133	6340	1527.18	5643.16	1638.62	1829.38	0.258	0.288
NS4	895	7520			2628.00	2933.94	0.349	0.390
NS8	2255	10820			229.67	338.70	0.021	0.031
NS9	1900	14060	2306.66	9115.52	1807.93	2666.21	0.128	0.189
NS10	1279	12790			4568.77	6737.70	0.357	0.527

The M–N interaction curves (Figures 4a and 4b) corroborate the observed results. For noncompact sections, Model III showed better alignment with the experimental data, although still conservatively. For slender sections, however, both models significantly underestimated the resistance measured in the tests, reflecting the limitations in representing the combined effect of high compression and local elastic buckling — precisely the shortcoming highlighted by Uy [9]. In summary, although Model III proves to be more representative of the behavior of composite columns under combined bending and compression, its performance is still limited in cases of high slenderness. This conservatism, while aligned with the normative purpose, underscores the need for advances in national design criteria, particularly regarding the consideration of post-buckling effects in slender sections.



(a) Noncompact section (b) Slender section

Figure 4. Uniaxial combined bending and compression interaction diagram – M–N

5 Conclusion

The results obtained confirm that the computational tool developed in MATLAB could apply Calculation Models I and III, recently incorporated into NBR 8800:2024, to assess the combined bending and compression resistance of concrete-filled rectangular composite columns. Comparisons with experimental data from the literature demonstrated reasonable consistency, albeit with a conservative trend for slender sections, reflecting the cautious nature of the normative models. The application of the tool to commercial profiles also highlighted its ability to capture variations in section classification and design criteria depending on the bending axis. It is recommended, however, to expand the database of experimental tests, particularly for noncompact and slender sections, to further refine the calculation models adopted by the code. Future studies should consider adjustments for post-buckling effects to improve the representation of structural behavior and provide support for future code revisions.

References

[1] Lai, Z., Varma, A. H., Zhang, K. Noncompact and slender rectangular CFT members: Experimental database, analysis, and design. *Journal of Constructional Steel Research*, 101, 455–468, 2014.
[2] Han, W., Wang, Y. High-strength square concrete-filled steel tube (HS-SCFT) beam-columns under cyclic loading: Experimental database, modeling, and analysis. *Structures*, 72, 108247, 2025.
[3] Ibáñez, C., Hernández-Figueirido, D., Piquer, A. Evaluation of Eurocode 4 and AISC for composite columns. *Journal of Constructional Steel Research*, 2021.
[4] Lai, Z., Varma, A. H. Effective stress–strain relationships for analysis of noncompact and slender filled composite (CFT) members. *Engineering Structures*, 124, 457–472, 2016.
[5] Associação Brasileira de Normas Técnicas. NBR 8800:2024 – Projeto e execução de estruturas de aço e de estruturas mistas aço–concreto de edifícios. Rio de Janeiro, 2024.
[6] AISC. Specification for Structural Steel Buildings. AISC 360–22. Chicago, IL, USA: AISC; 2022.
[7] Eurocode 4. Design of Composite Steel and Concrete Structures – Part 1-1: General rules and rules for buildings. EN 1994-1-1, CEN, Brussels, 2004.
[8] GB 50936. Technical Code for Concrete-Filled Steel Tube Structures. Beijing, China, 2014.
[9] Uy, B. Strength of concrete filled steel box columns incorporating local buckling. *Journal of Structural Engineering, ASCE*, 126(3), 341–352, 2000.
[10] MATLAB M. The language of technical computing. The MathWorks, Inc., 2023. Available at: http://www.mathworks.com.
[11] Mathematica. Mathematica Software, Version 14.0. Wolfram Research, Inc., Champaign, IL, 2024.
[12] Tuper. Tabela Técnica de Tubos. Tuper S/A, 2019.
[13] Protubsa. Catálogo Técnico de Tubos Estruturais. Grupo Bianco, 2025.
[14] Associação Brasileira de Normas Técnicas. NBR 6118:2023 – Projeto de estruturas de concreto — Procedimento. Rio de Janeiro, 2023.